J Mater Sci (2011) 46:2922–2927
DOI 10.1007/s10853-010-5167-z

A modified Johnson–Cook model for 30Cr2Ni4MoV rotor steel over a wide range of temperature and strain rate

Y. P. Wang · Chun-jie Han · Can Wang · Shi-ke Li

Received: 31 October 2010 / Accepted: 6 December 2010 / Published online: 29 December 2010

Abstract The compressive behaviors of 30Cr2Ni4MoV rotor steel were investigated at the temperatures from 1223 to 1523 K and strain rates from 0.001 to 0.1 s^{-1}. A modified Johnson–Cook (JC) model was proposed to describe the compressive behaviors of the studied alloy steel. In the modified JC model, the coupling effects of strain, strain rate, and deformation temperature were considered. Comparisons between the predicted stress–strain values by the modified JC model and measured ones indicate a good agreement, which confirms that the modified JC model is valid for the predicting the flow stress of 30Cr2Ni4MoV rotor steel over a wide range of temperature and strain rate.

Introduction

During the hot forming process of metals and alloys, the materials are subjected to complex time, strain, strain rate, and temperature histories in industrial forming processes. The hardening and softening mechanisms are both significantly affected by the temperature and strain rate. So, material flow behaviors during hot formation process is often complex. Constitutive equations should mathematically describe the deformation behavior of materials as a function of strain, strain rate, and temperature. Therefore, the construction of constitutive equations is highly complex, and frequently the valid strain range of application is very short. In order to ensure a valid numerical simulation of the hot forming processes of metals and alloys, a precise constitutive model describing the dynamic mechanical behavior of materials is prerequisite. Generally, an ideal plasticity model for metals and alloys should be able to accurately describe the material properties such as strain-rate dependence, forming temperature dependence, strain and strain-rate history dependence, work hardening or strain-hardening behavior (both isotropic and anisotropic hardening) [1–5].

In recent years, a large number of constitutive models have been proposed to describe the sensitivity of the flow stress to the strain, strain rate and deformation temperatures in commercial hot working applications [1–17]. Slooff et al. [2] established a strain-dependent constitutive relationship for three wrought magnesium alloys based on the hot uniaxial compression tests of over wide ranges of temperatures and strain rates were used for a strain-dependent constitutive analysis. It appeared that the apparent activation energy for deformation decreased with increasing the alloying content in these alloys. The constitutive parameters obtained were used to predict flow stresses at given strains and the results were in good agreement with experimental measurements. Khoddam and Hodgson [6] discussed the problem of model selection for representing the hot deformation behaviors of materials, and a heuristic approach was applied to define the merits for the model selection problem. They used a model library including some nested linear and non-linear models to capture the competing effects of hardening and softening during hot deformation. Lin et al. [7] proposed established the flow stress constitutive equations of the work hardening-dynamical recovery period and dynamical recrystallization period for 42CrMo steel, respectively, based on the classical stress-dislocation relation and the kinematics of

Y. P. Wang (✉) · C. Wang · S. Li
School of Chemical Engineering, Inner Mongolia Polytechnic University, Huhhot 010051, China
e-mail: ypwang68@163.com

C. Han
Inner Mongolia Vocational College of Chemical Engineering, Huhhot 010070, China

the dynamic recrystallization. By compensation of strain and strain rate, one new model to describe the relationships of the flow stress, strain rate and temperature of 42CrMo steel at elevated temperatures [8]. In addition, this modification method by strain compensation is useful for the aluminum alloy [9]. Considering the coupling effects of strain rate–temperature–strain, a combined Johnson–Cook and Zerilli–Armstrong (JC–ZA) model, and a modified JC model were developed to describe the relationship of the flow stress, strain rate and forming temperature for a typical high-strength alloy [10, 11]. Also, some other researchers [18–22] developed an artificial neural network (ANN) model to predict the hot deformation behavior of the alloy or metals and their results show that the ANN model can efficiently and accurately predict hot deformation behavior of alloys or metals.

Although the great progresses in the developments of material constitutive models have been made, the physical models are still not advanced enough to account for the whole complexity of the dynamic response of metals. In this study, the effects of strain rate and deformation temperature on the compressive behaviors of 30Cr2Ni4MoV rotor steel were investigated by uniaxial compression tests. A modified Johnson–Cook model for 30Cr2Ni4MoV rotor steel over a wide range of temperature and strain rate was developed to describe the relationship of the flow stress, strain rate, and temperature. In this modified Johnson–Cook model, the coupling effects of strain, strain rate, and deformation temperature were considered.

Experiments and results

30Cr2Ni4MoV is widely used as the turbine rotor and disk materials of the nuclear power generation. The chemical composition of 30Cr2Ni4MoV is (wt%): 0.28C–1.85Cr–3.35Ni–0.42Mo–0.089V–0.22Mn–0.06Si–0.004P–0.002S–0.007Al–0.06Cu–0.004Sn–0.0044As–0.0009Sb. Cylindrical specimens were machined with a diameter of 10 mm and a height of 12 mm. In order to minimize the frictions between the specimens and die during hot deformation, the flat ends of the specimen were recessed to a depth of 0.1 mm deep to entrap the lubricant of graphite mixed with machine oil. The hot compression tests were performed on Gleeble-1500 thermo-simulation machine in the four different temperatures (1223, 1323, 1423, and 1523 K) and three different strain rate (0.001, 0.01, and 0.1 s^{-1}). As shown in Fig. 1, the specimens were heated to 1523 K at a heating rate of 10 K/s by thermo-coupled feedback-controlled AC current, and held for 5 min. Then, the specimens were cooled at 10 K/s to the forming temperature and held for 5 min at isothermal conditions before compression tests, in order to obtain the heat balance.

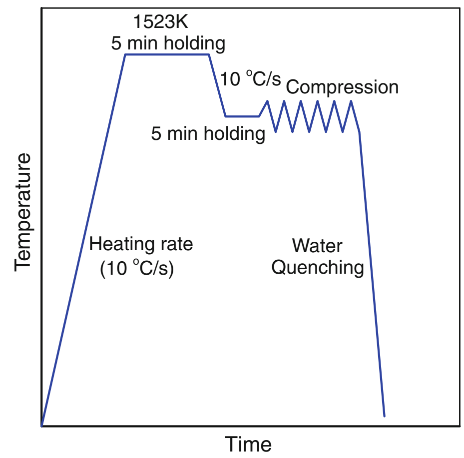

Fig. 1 Experimental procedure for hot compression tests

Figure 2 shows the typical true stress–strain curves obtained from uniaxial tensile tests of the studied alloy steel. It is noted that the flow stresses are strongly dependent on the deformation temperature and strain rate under all the tested conditions. The deformation resistance increases with the decrease of deformation temperatures for a given strain rate and decreases with the decrease of strain rates for a given deformation temperature. The material experiences simultaneous work hardening and dynamic recovery when they are deformed. The deformation mechanism associated with the isothermal uniaxial compression test is a thermally activated process, and the measured stress–strain curves represented the combined effects of strain, strain rate, and deformation temperature.

Constitutive equations for predicting flow stress

The stress–strain data obtained from hot compression tests under different strain rates and temperatures can be used to determine the material constants of constitutive equations. Among the empirical and semi-empirical models, Johnson–Cook model [23–25] is a most famous phenomenological flow stress model, and is successfully used for a variety of materials with different ranges of deformation temperature and strain rate [1]. It assumed that the material is isotropic, avoiding the traditional concept of yield surface in constitutive equation. Therefore, JC model has enjoyed much success because of its simplicity and the availability of parameters for various materials. The original Johnson–Cook model [23] can be expressed as:

$$\sigma = (A + B\varepsilon^n)(1 + C\ln\dot{\varepsilon}^*)(1 - T^{*m}) \quad (1)$$

where σ is the equivalent flow stress, ε is the equivalent plastic strain, A is the yield stress at reference temperature and reference strain rate, B is the coefficient of strain

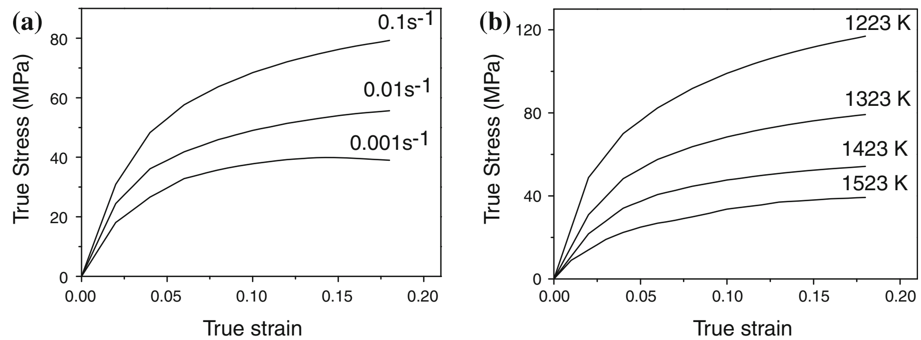

Fig. 2 Typical true stress–strain curves for 30CrNiMoV steel under different deformation conditions. **a** T = 1323 K; **b** $\dot{\varepsilon} = 0.1\mathrm{s}^{-1}$

hardening, n is the strain hardening exponent, C and m are the material constants which represent the coefficient of strain rate hardening and thermal softening exponent, respectively, $\dot{\varepsilon}^* = \dot{\varepsilon}/\dot{\varepsilon}_0$ is the dimensionless strain rate ($\dot{\varepsilon}$ is the strain rate, while $\dot{\varepsilon}_o$ is the reference strain rate), and T^* is the homologous temperature and expressed as $T^* = (T - T_r)/\ (T_m - T)_r$. Here, T is the absolute temperature, T_m is the melting temperature and T_r is the reference temperature.

It can be found that the original Johnson–Cook model requires fewer material constants and also few experiments to evaluate these constants. Johnson–Cook model assumes that thermal softening, strain rate hardening, and strain hardening are three independent phenomena and can be isolated from each other, i.e., the original Johnson–Cook model does not represent any thermal or strain-rate history effects, but is simple to implement and the parameters are readily obtained from a limited number of experiments. In general, the JC model represents a set of models that consider that the mechanical behaviors of material are the multiplication effects of strain, strain rate, and temperature. This form is simple and has a clear physical interpretation; however, JC model, together into the form of strain rate effect and temperature effect by multiplying simply with hardening effect, the coupling effects of strain, temperature and strain rate are omitted. Actually, the coupling effects of temperatures, strain rates, and temperature on the flow behaviors of the alloy steel should be considered. So, in this study a modified Johnson–Cook model is developed for the studied alloy steel, as shown in Eq. 2. The modified Johnson–Cook model considers the yield and strain hardening portion of the original Johnson–Cook model and the coupled effects of the temperature and strain rate on the flow behaviors.

$$\sigma = [A - B_0\exp(-B_1\varepsilon)][1 + (C_1 + C_2\varepsilon)\ln\dot{\varepsilon}^*] \times \exp[(\lambda_1 + \lambda_2 \ln\dot{\varepsilon}^*)(T - T_L)] \quad (2)$$

where A, B_0, B_1, C_1, C_2, λ_1, λ_2 are the material constants. σ is the equivalent flow stress, and ε is the equivalent plastic strain. T_L is the lowest temperature (1223 K) among the selected temperature range, while T is the deformation temperature. The meaning of $\dot{\varepsilon}^*$ is same as that of the original Johnson–Cook model.

Results and discussion

Based on the measured stress–strain data, the material constants of the modified Johnson–Cook model can be easily evaluated by the regression analysis with the experimental results. The followings are the steps to

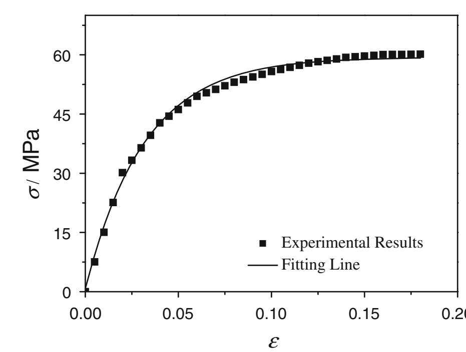

Fig. 3 Relationship between σ and ε to determine material A, B_0, and B_1

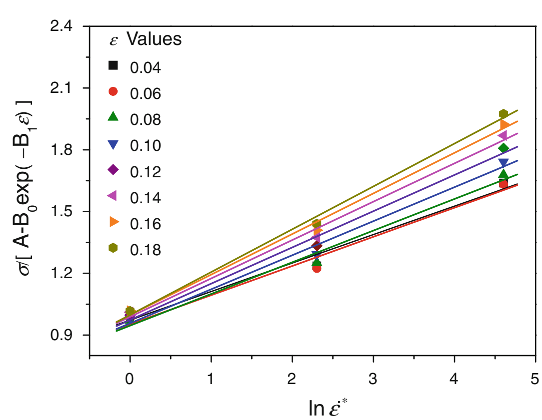

Fig. 4 Relationship between $\sigma/[A - B_0\exp(-B_1\varepsilon)]$ and $\ln\dot{\varepsilon}^*$ to determine material constant C

Table 1 Values of the material constant C corresponding to the different strains

ε	0.04	0.06	0.08	0.1	0.12	0.14	0.16	0.18
C	0.1384	0.14163	0.15387	0.16539	0.176	0.18637	0.19711	0.20806

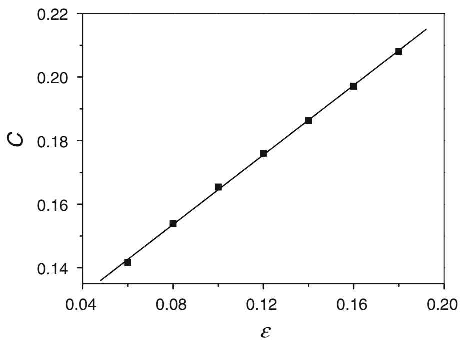

Fig. 5 Relationship between C and ε to determine material constants C_1 and C_2

determine the material constants. The reference strain rate ($\dot{\varepsilon}_o$) is selected as 0.001 s^{-1}.

Determination of material constants A, B_0, and B_1

When the deformation temperature (T) and strain rate ($\dot{\varepsilon}$) are 1223 K and 0.001 s^{-1}, respectively, Eq. 2 can be simplified as,

$$\sigma = A - B_0\exp(-B_1\varepsilon) \tag{3}$$

Based on the experimental results under the deformation temperature of 1223 K and strain rate of 0.0001 s^{-1}, the relationship between flow stress and strain can be obtained, as shown in Fig. 3. By means of the regression analysis with the experimental results, the values of A, B_0, and B_1 can be evaluated as 59.42 MPa, 58.64 MPa, and 31.40, respectively.

Determination of material constants C_1 and C_2

Similarly, taking the deformation temperature (T) as 1223 K, then Eq. 2 can be expressed as,

$$\sigma = [A - B_0\exp(-B_1\varepsilon)][1 + (C_1 + C_2\varepsilon)\ln\dot{\varepsilon}^*] \tag{4}$$

or

$$\frac{\sigma}{A - B_0\exp(-B_1\varepsilon)} = 1 + C\ln\dot{\varepsilon}^* \tag{5}$$

where C is the strain-dependent material constant, and $C = C_1 + C_2\varepsilon$.

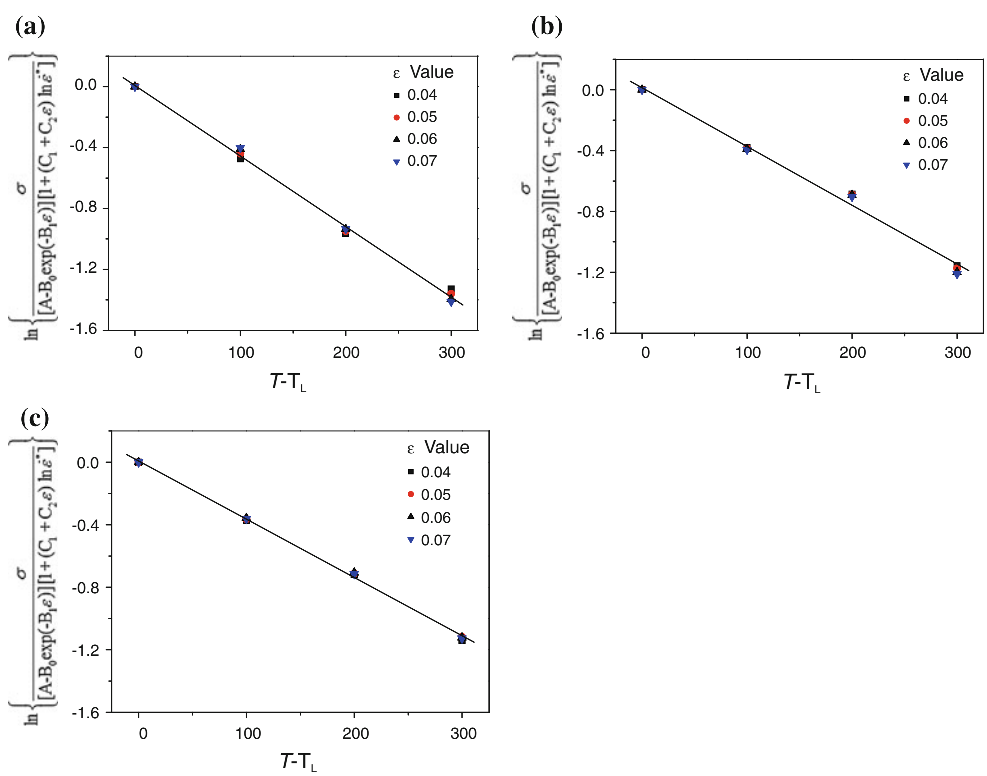

Fig. 6 Relationship between $\ln\left\{\frac{\sigma}{[A-B_0\exp(-B_1\varepsilon)][1+(C_1+C_2\varepsilon)\ln\dot{\varepsilon}^*]}\right\}$ and $T - T_L$ for different strain rate: **a** $\dot{\varepsilon}^* = 1$; **b** $\dot{\varepsilon}^* = 10$; **c** $\dot{\varepsilon}^* = 100$

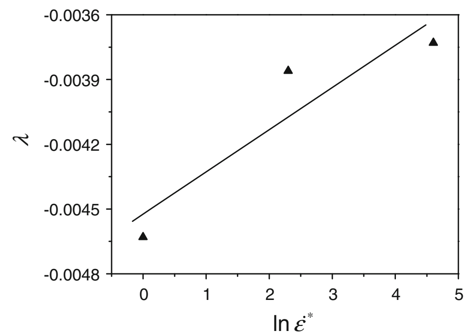

Fig. 7 Relationship between λ and $\ln\dot{\varepsilon}^*$ to determine material constants λ_1 and λ_2

When the deformation temperature is 1223 K and the strains is taken from 0.04 to 0.18 with the interval of 0.02, the relationship between $\sigma/[A - B_0\exp(-B_1\varepsilon)]$ and $\ln\dot{\varepsilon}^*$ can be obtained, as shown Fig. 4. Then, eight values of the material constant C corresponding to the different strains (shown in Table 1) can be evaluated as by linear fitting method. It is noted that all the fitting lines are shown in Fig. 4.

Obviously, the material constant C is a function of strain, and $C = C_1 + C_2\varepsilon$. From plots C–ε (Fig. 5), the values of material constants C_1 and C_2 can be linearly fitted as 0.10076 and 0.50777, respectively.

Determination of material constants λ_1 and λ_2

First, one strain rate-dependent material parameter, λ, is introduced, and λ is equal to $\lambda_1 + \lambda_2\ln\dot{\varepsilon}^*$. For a given strain rate, the material parameter, λ, can be considered as one material constant. Then, Eq. 2 can be expressed as,

$$\sigma/\{[A - B_0\exp(-B_1\varepsilon)][1 + (C_1 + C_2\varepsilon)\ln\dot{\varepsilon}^*]\} = e^{\lambda(T-T_r)} \tag{6}$$

Taking the logarithm of both sides of Eq. 6 gives

$$\ln\left\{\frac{\sigma}{[A - B_0\exp(-B_1\varepsilon)][1 + (C_1 + C_2\varepsilon)\ln\dot{\varepsilon}^*]}\right\} = \lambda(T - T_r) \tag{7}$$

For different strains, strain rates and deformation temperatures, the relationships between

Table 2 Material constants for modified Johnson–Cook equation for 30CrNiMoV steel

Parameters	A (MPa)	B_0 (MPa)	B_0	C_1	C_2	λ_1 (K^{-1})	λ_2 (K^{-1})
Value	59.42	58.64	31.40	0.10076	0.50777	−0.0045	0.00020

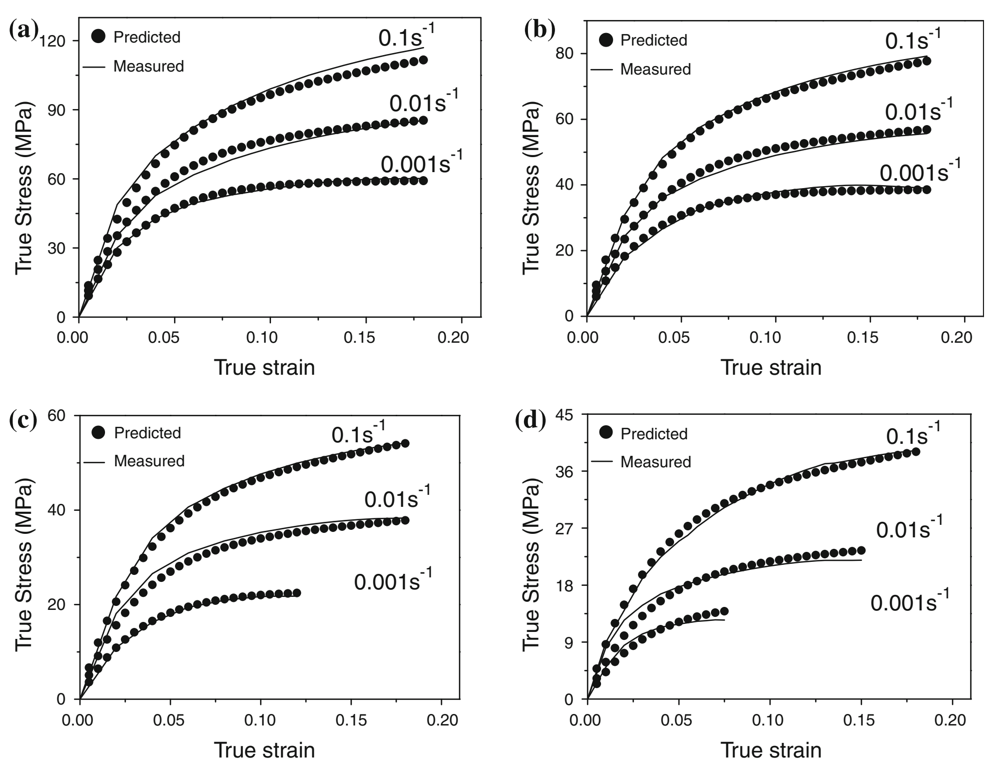

Fig. 8 Comparisons between predicted and measured flow stress cures of 30Cr2Ni4MoV rotor steel with the temperatures of **a** 1223 K; **b** 1323 K; **c** 1423 K; **d** 1523 K

$\ln\left\{\frac{\sigma}{[A-B_0\exp(-B_1\varepsilon)][1+(C_1+C_2\varepsilon)\ln\dot{\varepsilon}^*]}\right\}$ and $(T-T_L)$ can be obtained, as shown in Fig. 6. Then, $\lambda_{(\dot{\varepsilon}^*=1)}$, $\lambda_{(\dot{\varepsilon}^*=10)}$, and $\lambda_{(\dot{\varepsilon}^*=100)}$ can be evaluated as −0.00373, −0.00386, and −0.00463, respectively, when the dimensionless strain rates ($\dot{\varepsilon}^*$) are 1 (Fig. 6a), 10 (Fig. 6b), and 100 (Fig. 6c). Finally, λ_1 and λ_2 can be computed as −0.00452 K^{-1} and 0.00020 K^{-1} from $\lambda-\ln\dot{\varepsilon}^*$ plot (shown in Fig. 7).

Comparisons between the measured and predicted flow stress

Based on the above analysis, the material constants for the modified Johnson–Cook equation can be summarized in Table 2. Figure 8 shows comparisons between the measured and predicted results by the modified Johnson–Cook model of 30Cr2Ni4MoV rotor steel under four different temperatures and three different strain rates. It indicates the predicted flow stresses well agree with the measured values. The results indicate that the modified Johnson–Cook model can give an accurate and precise estimate of the flow stress for 30Cr2Ni4MoV rotor steel, and can be used to analyze the problems during metal forming process.

Conclusions

The hot compressive characteristics of 30Cr2Ni4MoV rotor steel have been investigated over a practical range of temperatures and strain rates. Based on experimental stress–strain data, a modified Johnson–Cook model, which considers not only the yield and strain hardening phenomenon, but also the coupling effects of the temperature and strain rate, is proposed to predict the flow stress. Comparisons between the experimental and predicted results were carried out and confirmed that the developed constitutive equations can presented an accurate and precise estimate of the flow stress for 30Cr2Ni4MoV rotor steel.

References

1. Lin YC, Chen XM (2010) Mater Des. doi:10.1016/j.matdes.2010.11.048
2. Slooff FA, Zhou J, Duszczyk J, Katgerman L (2008) J Mater Sci 43:7165. doi:10.1007/s10853-008-3014-2
3. Lin YC, Chen MS (2009) Mater Sci Eng A 501:229
4. Lin YC, Chen MS, Zhong J (2008) Comput Mater Sci 44:316
5. Lin YC, Chen MS (2008) J Mater Sci 44:835. doi:10.1007/s10853-008-3120-1
6. Khoddam S, Hodgson PD (2010) Mater Des 31:2011
7. Lin YC, Chen MS, Zhong J (2008) Mech Res Commun 3:142
8. Lin YC, Chen MS, Zhong J (2008) Comput Mater Sci 42:470
9. Lin YC, Xia YC, Chen MS (2010) Comput Mater Sci 50:227
10. Lin YC, Chen XM (2010) Comput Mater Sci 49:628
11. Lin YC, Chen XM, Liu G (2010) Mater Sci Eng A 527:6980
12. Han YF, Zeng WD, Zhao YQ, Zhang XM, Sun Y, Ma X (2010) Mater Des 31:4380
13. Yan LM, Shen J, Li ZB, Li JP, Yan XD, Mao BP (2010) Chin J Nonferrous Met 20:1296
14. Mcqueen J, Ryan ND (2002) Mater Sci Eng A 322:43
15. Jesús C, Ignacio R, Manuel C, Oscar AR (2010) J Mater Sci 45:5522. doi:10.1007/s10853-010-4610-5
16. Lin YC, Liu G (2010) Comput Mater Sci 48:54
17. Mandal S, Rakesh V, Sivaprasad PV, Venugopal S, Kasiviswanathan KV (2009) Mater Sci Eng A 500:114
18. Odejobi OA, Umoru LE (2009) Afr J Math Comput Sci Res 2:104
19. Hakamada M, Watazu A, Saito N, Iwasaki H (2008) J Mater Sci 43:2066. doi:10.1007/s10853-008-2474-8
20. Ji GL, Li FG, Li QH, Li HQ, Li Z (2010) Comput Mater Sci 48:626
21. Lin YC, Zhang J, Zhong J (2008) Comput Mater Sci 43:752
22. Kalaichelvi V, Sivakumar D, Karthikeyan R, Palanikumar K (2009) Mater Des 30:1362
23. Johnson GR, Cook WH (1983) In: Proceedings of the 7th international symposium on ballistics, p 541
24. Johnson GR, Cook WH (1985) Eng Fract Mech 21:31
25. Rohr I, Nahme H, Thoma K, Andreson CE Jr (2008) Int J Impact Eng 35:811